Environmental Challenges 11 (2023) 100708

Contents lists available at ScienceDirect

Environmental Challenges

journal homepage: www.elsevier.com/locate/envc

Multi-layer perceptron's neural network with optimization algorithm for greenhouse gas forecasting systems

Ashok Kumar Nanda [a], Neelakandan. S [b,*], Sachi Gupta [c], Angel Latha Mary Saleth [d], Ramya. S [e], Siripuri Kiran [f]

[a] Department of CSE, B V Raju Institute of Technology, Narsapur Medak, Telangana, India
[b] Department of Computer Science and Engineering, R.M.K Engineering College, Chennai, India
[c] Department of Information Technology, IMS Engineering College, Ghaziabad, India
[d] Department of Computer Science and Business Systems, Sri Eshwar College of Engineering, India
[e] Department of Electronics and Communication Engineering, R.V.College of Engineering, India
[f] Department of CSE(Networks), Kakatiya Institute of Technology & Science, Warangal, Telangana 15, India

ARTICLE INFO

Keywords:
Co2 emission
Forecasting
Machine-learning algorithms
Greenhouse gas (GHG)
Multi-layer perceptron's neural network (MPNN)
Modified coyote optimization algorithm (MCOA)

ABSTRACT

China, India, and the United States consume the most energy and emit the most CO2. According to datacommons.org, India's CO2 emission is 1.80 tnes per capita, which is harmful to living beings: hence, this study exhibits India's harmful CO2 emission effect and forecasts CO2 emission for the next ten years using univariate time-series data from 1980 to 2019. A multilayer perceptron is used in this study to analyse 2099 experimental data of binary systems made up of CO2 and ionic liquids and predict solubility. 33 different types of ionic liquids are represented in the dataset, which spans a wide variety of solubilities, pressures, and temperatures. In recent decades, greenhouse gas (GHG) emissions have caused air pollution and environmental problems in several countries. A precise prediction is essential for managing and planning for the decrease of greenhouse gas emissions. Furthermore, the Modified Coyote Optimization Algorithm was used to extract required properties. The empirical data revealed that predictions obtained from Multi-Layer Perceptron's Neural Network (MPNN) were more accurate than those derived from other models. The MPNN-MCOA identified a link between CO2 emissions, economic growth, and entrepreneurship. Government, personal liberty, education, and pollution all have a negative correlation. We conclude by emphasising the critical role of machine learning in achieving carbon neutrality, from global-scale energy management to the revolutionary potential of atomic-scale MPNN-MCOA simulations for application development. As a result, one of the most reliable approaches for estimating greenhouse gas (GHG) emissions from agricultural regions and companies was recommended: the MPNN-MCOA model. The Artificial neural network is trained with three input combinations with three combinations of thermodynamic variables such as temperature (T), pressure (P), critical temperature (Tc), critical pressure, the critical compressibility factor (Zc), and the acentric factor (w). Moreover, the proposed MPNN–MCOA model demonstrates an improvement in the forecasting accuracy obtained from the LSTM, KNN, CNN, and MPNN–MCOA models by 50.82%, 34.91%, 44.19%, and 29.77% decrease in mean square error, respectively.

1. Introduction

In recent decades, the impact of greenhouse gas emissions on the atmosphere has prompted significant technical advancements. This is due to the fact that our planet's environmental challenges not only affect our natural environment, but also human health and the global economy. Presently, the primary cause of global warming and climate change is carbon dioxide produced by the combustion of fossil fuels for energy generation. Numerous businesses have acknowledged the need to limit carbon dioxide emissions. Industrial processes have therefore adopted methods to limit the quantity of carbon dioxide discharged into the atmosphere (Fernández et al., 2018).

Current CO2 capture research focuses on three primary alternatives: precombustion, oxy-combustion, and postcombustion . Postcombustion capture has been utilised extensively for CO2 collection in natural gas, refinery off-gases, and synthesis gas processing (Kjellstrom, 2016). Modern postcombustion technologies consider amines such as monoethanolamine, diethanolamine, methyldiethanolamine, and 2-amino-2-, ethyl1-propanol (Keith et al., 2018). However, the amine-based afterburning approach has a number of disadvantages, including the pro-

* Corresponding author.
E-mail address: snk.cse@rmkec.ac.in (Neelakandan. S).

https://doi.org/10.1016/j.envc.2023.100708
Received 20 November 2022; Received in revised form 1 March 2023; Accepted 16 March 2023

duction of corrosive byproducts due to amine degradation, solvent loss, and a high energy requirement for sorbent regeneration (Romeo et al., 2020).

This new category of nonaqueous fluids is comprised of an asymmetric organic cation and an organic or inorganic anion. Generally speaking, ionic liquids are organic salts that are liquid at normal temperature. Its characteristics include great thermal stability, low vapour pressure and toxicity, a low melting point, and straightforward recycling. Moreover, their physical and chemical properties can be manipulated by altering the cation. Ionic liquids require less energy to regenerate and eliminate captured CO2 than existing technology based on aqueous amines (Zeng et al., 2017). Because the burning of fossil fuels is the primary source of carbon dioxide (CO2), controlling CO2 emissions from energy consumption and economic expansion is a global challenge. In 2018, greenhouse gas emissions reached a new high of 33,1 billion tonnes, while global GDP expanded by 3.2%. China and the United States are the top two energy consumers and carbon emitters, with increases of 2.5% and 3.1%, respectively as a result of increased usage of fossil fuels to meet energy demand. This occurred despite the fact that CO2 emissions reached a two-year plateau between 2014 and 2016.

The correlation between emission observations and statistical hypotheses might not be perfect. The advantage of using MGPMs is that you may characterise an unidentified system with a small sample size and without making any statistical assumptions. Despite having access to massive amounts of data, only a small sample size is required to create trustworthy predictions. According to the World Resources Institute (WRI), around 76% of greenhouse gas emissions in 2018 were caused by the generation of electricity from fossil fuel-powered power plants and the consumption of energy in various industries. Agriculture is the second-largest sector (12%), after only industry (5,7%) and other (5,7%). Iran is also the world's eighth-largest emitter of greenhouse gases and the seventh-largest producer of carbon dioxide. The remaining 13% comes from agriculture, industry, and other sectors, accounting for 87% of the total. Since 2008, Iran's annual CO2 emissions have risen to more than 500 Mt (Mostafaeipour et al., 2022). The energy sector has been the focus of numerous studies (Shabani et al., 2021), since it has created the greatest amount of greenhouse gas emissions in recent years. This is because reducing greenhouse gas emissions is critical to preventing global warming and temperature increases.

Air pollution and greenhouse gas emissions endanger both human and environmental health. Planning for energy generation in green energy sectors, as well as the right planning required to meet economic goals and sustainable development, greenhouse gas emissions forecast Delegates at the COP26 climate change meeting in 2021 addressed methods to reduce greenhouse gas emissions on 28 fronts. It has been investigated to utilise machine learning to anticipate greenhouse gas emissions. People can then determine for themselves how to reduce and regulate their greenhouse gas emissions (Dwivedi et al., 2022).

Numerous studies have been conducted in recent years using a range of methodologies and models to forecast GHG emissions with varying degrees of accuracy. This situation exists because forecast accuracy is important in the field of forecasting research. Several studies looked at a range of enterprises that generated greenhouse gas to reduce emissions, various levels of forecast accuracy are utilised in conjunction with machine learning technologies. There is a plethora of evidence were also utilised to gauge the forecast's accuracy. To forecast China's carbon emission reduction targets, the publication (Niu et al., 2020) provides a case study forecasting Carbon emission will be decreased by 2030 by using machine learning algorithms and an algorithm-coupled strategy. They were mentioned in relation to the Chinese leadership. A different study (Yang and O'Connell, 2020) employed the ARIMA modelling technique to project CO2 emissions for the Chinese aviation industry over the next five years based on the amount of fuel required for travel. In a second study, utilising data from 2015 to 2019, The Radial Basis Function (RBF) network model was used to do the assessment anticipate how much greenhouse gas emissions the Iranian vehicle sector will release in 2030. In a following study, the LSTM, KNN, and CNN algorithms were utilised separately (Javadi et al., 2021). The study (Samal et al., 2021) assessed CO2, N2O, CH4, and fluorinated gas emissions using SVM, ANN, and deep learning algorithms. The accuracy of these approaches was evaluated using five distinct prediction accuracy criteria. The ANN algorithm was utilised in a study (Bakay and Agbulut, 2021) on CO2 emission reduction in Canada's industrial sectors to forecast CO2 emissions in 2035. In a separate study, CO2 and N2O emissions from agricultural practises were calculated using the accuracy of their emission estimates was evaluated (Olanrewaju and Mbohwa, 2017). The ARIMA approach, along with other techniques, was used to project CO2 emissions for China, India, and the United States for the year 2030 (Hamrani et al., 2020).

Another factor contributing to the high increase in CO2 the exponential growth in the number of automobiles on the road is one of the leading causes of air pollution. This is due to global population expansion. The number of autos on the road is expected to triple by 2050. (Ahmadi, 2019). As a result, a variety of specific activities must be done by government officials and decision-makers to offset the negative effects of increased CO2 emissions. Projecting CO2 emissions is also a crucial step in educating the public about environmental issues. The study included a thorough investigation of four two models based on machine learning and two statistical models, and one deep learning model in order to anticipate CO2 emissions over time series. Nine parameters were used to determine which model will provide the best accurate projections of CO2 emissions until 2030. After conducting extensive research on the outcomes of a large number of fictitious occurrences, our team developed a few models that provide reasonably accurate forecasts. The data used shows how CO2 emissions have increased over the last four decades.

In recent years, the usage of artificial neural networks (ANN) has been increasingly prevalent in a variety of sectors, including medical applications, pharmaceutical sciences, engineering, banking, and social media, among others. One of its major advantages is its capacity to quickly adapt to its surroundings (data, tasks, and so on). During training, it can also discover redundant and noisy variables. To anticipate traffic arrival delays using ANN, we choose the multilayer perceptron (MLP) due to its superior performance and reliability. MLP can model extremely nonlinear functions and has been found to be effective when supplied with new, unseen data, unlike other statistical methods. The MLP has been utilised for a wide range of applications, including prediction, function approximation, and pattern categorization. MCOA was superior to COA in terms of its capacity to locate solutions of a higher quality, its search stability, and its convergence speed. In addition, five other metaheuristic algorithms consisting of biogeography-based optimization (BBO), genetic algorithm (GA), particle swarm optimization algorithm (PSO), sunflower optimization (SFO), and salp swarm algorithm (SSA) were applied to the same problem for the purpose of evaluating ICOA's performance. The comparisons of results have also demonstrated the exceptional performance of MCOA, as it was able to discover significantly superior results than these methodologies, particularly SFO, SSA, and GA.

In this paper, the predictions obtained using the Multi-Layer Perceptron's Neural Network (MPNN) were more accurate than those obtained using other models. The MPNN-MCOA found a link between CO2 emissions, economic growth, and entrepreneurial opportunity. Governance, personal freedom, education, and pollution all have a negative association. To accelerate the achievement of carbon neutrality, we describe the critical role that machine learning plays in all aspects of global energy management, from the ground breaking screening of advanced energy materials in vast chemical spaces to the revolutionary atomic-scale simulations of MPNN-MCOA, which have a promising future. As a result, the MPNN-MCOA model is proposed as one of the most acceptable models for estimating soil greenhouse gas (GHG) emissions from an agricultural area and industrial areas.

The remainder of the work is organised as follows: in Section 2, we give a summary of past research that has addressed the privacy problem and proposed remedies. Section 3 describes the proposed algorithm and privacy analysis. Section 4 reports on performance evaluations. Section 5 concludes the report and presents our next work.

2. Literature survey

Fang et al. (2020) proposed a perfect random forest model for the accurate prediction of an infectious diarrhoea outbreak, considering several meteorological circumstances. He compared the model he was presenting against ARIMA and ARIMAX and discovered that the RF model outperformed the ARIMA model. The ARIMA model had MAPE values as high as 30%, whereas the RF model had MAPE values as high as 50%.

Wang et al. (2020) proposed that precise data on the quantity of CO2 emitted by automobiles should be used to design efficient carbon mitigation methods. The data trend on carbon emissions differs between China, the United States, and India. The data on car emissions in the United States shows an erratic increase and fall. In this study, the author presents a method for improving data accuracy. Using ARIMA and BPNN, this strategy This may result in a reduction in the residual error of the MNGM model. It can also help to reduce the model's prediction error. Carbon emissions in the United States are likely to fall during the next few decades.

Quear et al. (2019) Discussed Environmentally and economically, it is of the utmost importance to estimate the solubility of carbon dioxide in ionic liquids with the aid of trustworthy models. In this regard, the objective of the current study is to evaluate the performance of two data-driven techniques, namely multilayer perceptron (MLP) and gene expression programming (GEP), for predicting the solubility of carbon dioxide (CO2) in ionic liquids (ILs) as a function of pressure, temperature, and four thermodynamically parameters of the ionic liquid. To create the aforementioned methodologies, 744 experimental data points collected from 13 ILs were employed (80% for training and 20% for validation). The MLP algorithm was optimized using two backpropagation-based techniques, namely Levenberg–Marquardt (LM) and Bayesian Regularization (BR).

Song et al. (2020) Proposed A database encompassing 10,116 measurements of CO2 solubility in various ionic liquids (ILs) at varying temperatures and pressures is created. Using group contribution (GC) methods, this database is utilized to establish a correlation between CO2 solubility and IL structure, temperature, and pressure. Two distinct machine learning approaches, artificial neural network (ANN) and support vector machine (SVM), are used to construct GC models. Estimated MAE and R2 for the 2023 test set are 0.0202 and 0.9836 for the ANN-GC model and 0.0240 and 0.9774 for the SVM-GC model.

Cao, et al. (2019) Stock price research focuses on complex networks and volatility trends. Previous studies predicted price changes based on historical data for a certain stock, rarely considering price co-movement across multiple stocks. They used networks and machine learning to predict stock prices. S&P 500, NASDAQ, and DJIA.Price volatility patterns weighed on networks. KNN and SVM used the topology properties of each combination of symbolic patterns to forecast the volatility characteristics of a given stock for the upcoming trading day. Cross-validation and search can determine the best models for these two algorithms. The testing dataset's three indexes are over 70% accurate. Prediction-wise, SVM beat KNN.

Magazzino et al. (2023) investigated the association between renewable energy technology and Germany's GDP per capita, biomass energy use, and CO2 emissions. To discover the relationship, they developed a new model, the Quantum Model, which was integrated with machine learning algorithms. Because of this, they think that biomass energy is a good way to cut CO2 emissions, but that renewable energy is a better way.

Lepore et al. (2017), the most recent EU rule on CO2 emissions requires ship owners to install CO2 emissions monitoring and reporting systems. They will be better positioned to make business decisions if they have these answers. Because of the difficulties involved in utilising ship-provided navigation information. Because of the complexities of ship navigational data, this is the case. An in-depth investigation of the various regression techniques that could be applied to ship navigation data is undertaken here. The two basic goals of this project are to identify viable methodologies and models for analysing the ship's CO2 emissions and to create a forecasting model.

Daryayehsalameh et al. (2021) Proposed the solubility of CO2 in 1-n-butyl-3-methylimidazolium tetrafluoroborate ([B*mim*][BF4]) is estimated using six distinct artificial intelligence (AI) techniques, including four artificial neural networks (ANN), support vector machines (LS-SVM), adaptive neuro-fuzzy interface system, and support vector machines (SVM) (ANFIS). The cascade feed-forward neural network was determined to be the best model for the subject under consideration. This model accurately predicts all experimental datasets with AARD = 6.88%, MSE = 8 104 and R2 = 0.98808%.

Li et al. (2018) studied the amount of CO2 emitted in the Beijing-Tianjin-Hebei region because the entire nation is powered by fossil fuels. To improve the extreme learning machine technique, SVM-ELM, a novel forecasting strategy that leverages the support vector machine's core algorithmic component was developed. When using grey prediction, to calculate the regional carbon footprint, they discovered that energy use had a major impact on total carbon emissions. As a result, the grey prediction approach was determined to be a good choice. Grey prediction was used in the first stage of the approach to estimate CO2 emissions between 2017 and 2030. The forecast findings were then fed into SVM. Thus, revealed that these techniques outperformed both SVM and ELM in accurately predicting future carbon emission levels (ELM). They predicted that by 2027, more than 97 million metric tonnes of CO2 emissions will have been produced, and they asked the government to promote the use of renewable energy.

Wang and Ye (2017) aimed to determine the rate of carbon emissions between the years 2014 and 2020 by considering the using fossil fuels weighted against the total amount of energy consumed. They calculated how slow, medium, and fast economic growth would affect CO2 emissions and came up with a solution based on ARIMA and a non-linear grey prediction model.

Shaikh et al. (2017) developed a paradigm for Turkey's current and future water and carbon footprints. Based on 1990–2013, the ARIMA model estimated energy output for 2030, The three potential outcomes—business as usual, enactment of the government's plan, and advancement of renewable energy—were reduced to a manageable number using the ARIMA model. 6.67 × 1011 gallons and 2.05 × 108 kg, respectively, are the estimated water and carbon footprints for 2030. In comparison to the baseline scenario of the government plan, these statistics show decreases of 7.5% and 28%, respectively.

Mesbah et al. (2018) In this study, the solubility of CO2 and supercritical (SC) CO2 in 20 ionic liquids (ILs) of various chemical families was predicted over a wide range of pressure (0.25–100.12a MPa) and temperature (278.15–450.49a K) using a robust machine learning method of multi-layer perceptron neural network (MLP-NN). With R2 of 0.9987, MSE of 0.6293, and AARD% of 1.8416, the generated model accurately predicted experimental values. Table 1 details some ANN models reported in the last 10 years to predict CO2 solubility in LIs.

3. Proposed system

CO2 emissions in India are increasing at an alarming rate, endangering the environment and, eventually, all living beings. Hence, reducing CO2 emissions should be the government and industry's top concern. We have CO2 emission time series data from 1980 to 2019 as well as some of its characteristics. Because this project required a univariate dataset, further data pre-treatment and cleaning were required to account for the missing values in the dataset. The data is organised into two columns: one for the years and another for the CO2 emissions in

Table 1
MLP-based models that estimate the solubility of binary mixtures composed of CO2 and ILs are described in detail.

Author	Year	Data Point Studied	Data Point Predicted	System	R2	Input	Np*
Ouaer et al. (2019)	2019	744	149	13	0.997	T, P, Mw, Tc, Pc, w	327
Song et al. (2020)	2020	10,116	2023	124	0.0202	51 group numbers, T and P	386
Daryayehsalameh et al. (2021)	2021	548	110	17	0.98684	T and P	25
Mesbah et al. (2018)	2018	1386	208	20	0.9987	Mw, Tc, Pc, T, P	261
Tatar et al. (2016)	2016	728	148	14	0.998	T, P, Tc, Pc, w	162
Sedghamiz et al. (2015)	2015	2930	440	39	0.9947	T, P, Tc, Pc, w	162

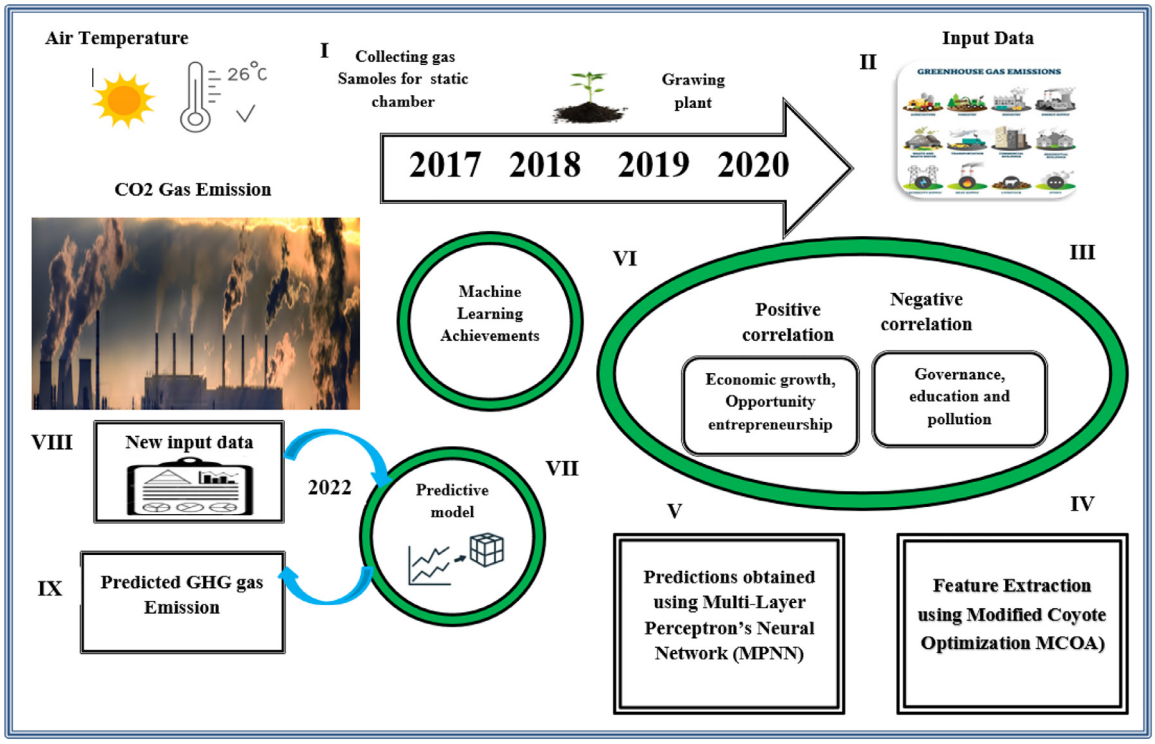

Fig. 1. Proposed MPNN-MCOA method.

metric tonnes. Fig. 1 depicts a block schematic of the proposed MPNN-MCOA approach.

3.1. Data collection and pre-processing

Statistics on Iran's greenhouse gas emissions and economic sectors that contributed were compiled from 1990 to 2018. At numerous power plants, electricity is generated and fossil fuels are used on electricity exports and imports, data on electricity generation over a 28-year period, data on greenhouse gas emissions (including carbon dioxide, nitrous oxide and fluorinated gases), and data on residential, public, and industrial energy consumption are included. The pace of increase in greenhouse gas emissions between 1990 and 2018. Data for this inquiry were provided by the Ministry of Energy and the Iranian Statistical Canter (Hosseinzadeh et al., 2021). Appendix A contains the data utilised in this study, and some of the GHG emission estimates used in this analysis may be found in the World Resources Institute database. The results of forecasting algorithms are used to improve estimates of greenhouse gas emission levels. Appendix A contains the raw data required to create the model for the most accurate outcome prediction.

3.2. Multilayer perception neural network architecture

A variety of strategies can be used when creating and implementing A neural network-based prediction model. The feedforward neural network structure and the back-propagation learning method have been used often in a number of scenarios. This, or a derivative of it, which was then put to use in a variety of other ways. Several people assert that experts in the field, identifying the appropriate network size for successful forecasting of real-world time series has proven difficult. In a neural network, regardless of the number of hidden layers, there will always be at least one input layer and one output layer. The particulars of the current scenario strongly influence the selection of elements to be used. Numerous methodologies, such as the polynomial time algorithm, the pruning algorithm, the canonical decomposition approach, and the network information criterion, have been developed to aid in the establishment of the best network topology. However, none of these techniques can ensure that the parameters will be optimal for every type of forecasting scenario.

According to the existing literature, there does not appear to be a systematic strategy to investigate these concerns. Many researchers in the field of artificial neural networks (ANN) used iterative methods to arrive at a practical solution to a problem, which is the primary reason of inequalities in the ANN literature. It is impossible to build the best neural network design using a single, consistent set of rules. The number of inputs, the number of hidden units, and the layout of these units into layers are frequently determined by trial and error or in advance, depending on the preferences of each designer. Occasionally, the project's goal demands may be allowed to dictate these specifics.

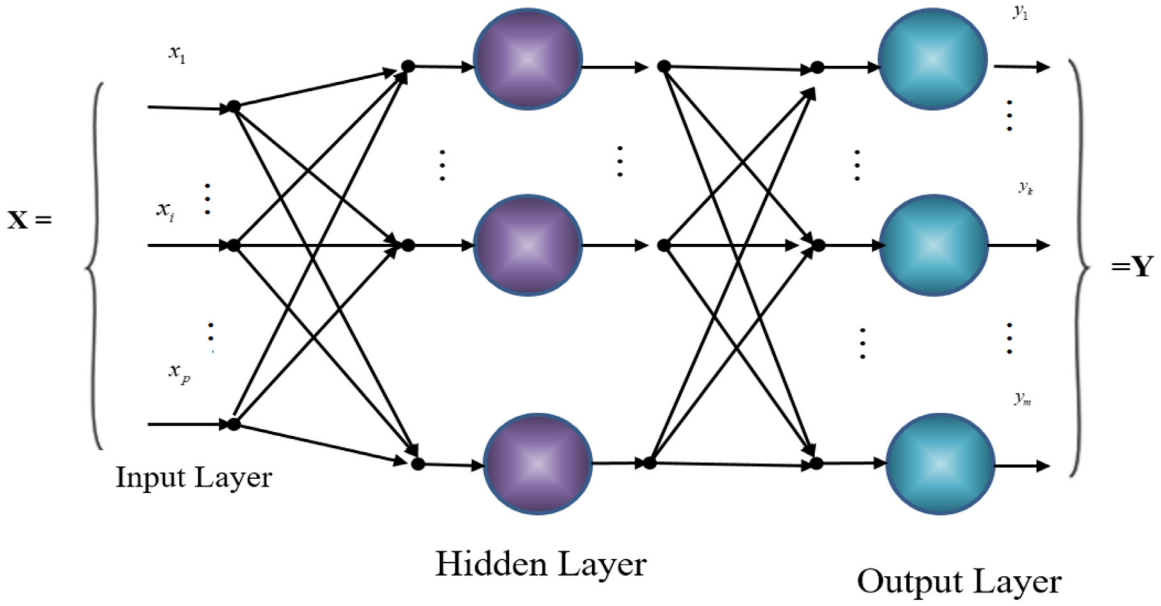

Fig. 2. An introduction to the multilayer perceptual neural network model.

The MLPNN approach consists of four steps:

- deciding on a variable
- Methodologies for instruction, evaluation, and formula verification
- Buildings and other structures
- Model validation and forecasting

The MLPNN model was developed for this study using Zaitun, a time series analysis tool. The variables for this experiment will be chosen by software. According to our findings, introducing an early termination limit can lessen the risk of MLPNN overfitting. Under this stopping scenario, the learner progressed over time through iterative training. Two universal rules determine halting conditions (i.e., mean square error value and mean square error change). These rules specify the amount of iterations to complete before using the learner's overfitting. Each test employs various models with varying layer combinations (input, hidden, and output layers), four activation functions, and a total of four activation functions (i.e., semilinear, sigmoid, bipolar sigmoid, and the hyperbolic tangent function).

3.3. Optimization process of coyote optimization algorithms

Before diving into the key steps of the Coyote Optimization Algorithm, it is critical to familiarise yourself with the following explanations (COA).

- Despite sharing a pack, each coyote has its own network of contacts and social roles. The social condition represents a prospective solution, and the fitness function value corresponding to the quality of the prospective solution is associated with the quality of the social condition.
- Each Mg group contains at least one coyote from the coyote population. As a result, the entire COA population is steps M_{co}, is M_{pop} (where $M_{gro}\ \ M_{pop} = M_{co} \times M_{gro}$)
- It is critical to evaluate the p^{th} coyotes and $Co_{p,gro}$ social environment and gro^{th} position within the pack (which is the $FF_{p,gro}$ of the solution).

Establishing a coyote colony

Step 1. Create initial coyote community

The first set of responses can be compared to the early coyote society, with each response reflecting a separate social situation to which each coyote was exposed. Each coyote pack, however, has its own initiation process, as illustrated below:

$$Co_{p,gro} = Co^{\min} + \gamma.(Co^{\max} - Co^{\min}) \quad p = 1, ..., M_{Co}, gro = 1, ..., M_{gro} \tag{1}$$

where $Co^{\min}$ and $Co^{\max}$ the equation has two solutions, one for each bound—lower and upper.

$$Co^{\min} = [\mathrm{var}_x^{\min}]; \quad x = 1, ..., M_{dv}$$
$$Co^{\max} = [\mathrm{var}_x^{\max}]; \quad x = 1, ..., M_{dv}\ \text{the}^{x^{th}} \tag{2}$$

where $\mathrm{var}_x^{\min}$and $\mathrm{var}_x^{\max}$ where and are the lowest and highest values of thex^{th} controlled variable.

Step 2. It is critical to examine a coyote's social environment while determining its fitness function value. It's similar to figuring out a solution's fitness function. A fitness function then compares possible new solutions which is frequently produced by combining an objective function and a penalty function. The fitness function ranks these features. An example of a typical fitness function in the context of an optimization problem is shown below:

$$FF_{p,gro} = OF_{p,gro} + PF. \sum_{n=1}^{N} (PT_{p,gro,n})^2 \tag{3}$$

Where, $PT_{p,gro,n}$is the penalty for breaching n^{th}a constraint of the p^{th} of the gro^{th} group group's solution is decided by an experience-based factor known as PF.

Local best solution is defined as the answer with the highest fitness function inside each group $Co_{best,gro}$.

Step 3. Consider the solutions of each group.

The modernization of new techniques is associated with the modernization of coyote status within each group. The COA locates new solutions near current ones Use a compromise response, a set of distances based on the closest best answer, a set of randomly selected answers, and a set of distances based on the closest best answer. The model below describes the specifics of the improved solution strategy.

$$Co_{p,gro}^{new} = Co_{p,gro} + \gamma(Co_{best,gro} - Co_{1.gro}) + \gamma(Co_{mid,gro} - Co_{2,gro}) \tag{4}$$

In Eq. (8), $Co_{1,gro}$and $Co_{2,gro}$ are two answers that were chosen at random in thegro^{th} taking into account a collection while $Co_{mid,gro}$ A company's approach to compromisegro^{th} group. As indicated by the following equation, the production of each option variable in the middle solution has two alternative outputs.

$$Co_{mid,gro} = \begin{cases} Var_{x,mid1}, & if\ M_{Co}\ is\ odd \\ Var_{x,mid2}, & else \\ x = 1, ...M_{dv} \end{cases} \quad (5)$$

Step 4. Examine the efficiency.

Consider the viability of any suggested changes. Fitness function analysis is used to rank the quality of new replies (3)

Step 5. Employing a selection mechanism.

Each coyote k now has two sets of social conditions, one for the current solution and one for the previous solution, $Co_{p,gro}$, As the economy and society evolve, new perspectives on age-old issues are required, $Co^{new}_{p,gro}$. The fitness function for the two alternative solutions is determined by the characteristics of the two social contexts, $FF_{p,gro}$ and $FF^{new}_{p,gro}$. If these parameters are followed, it should be able to maintain one social condition for every kth coyote.

$$Co_{p,gro} = \begin{cases} Co^{new}_{p,gro}, & if\ FF^{new}_{p,gro} \le FF_{p,gro}, \\ Co_{p,gro}, & else, \end{cases} \quad (6)$$

$$FF_{p,gro} = \begin{cases} FF^{new}_{p,gro}, & if\ FF^{new}_{p,gro} \le FF_{p,gro}, \\ FF_{p,gro}, & else. \end{cases} \quad (7)$$

Step 6. Create a completely new social state in every grouping during the sixth step.

Now, each team will approach the problem in its own special way Co^{new}_{gro} using a technique that yields random results The new tactic is illustrated by the following sample scenarios:

$$Co^{new}_{gro} = \left[Var^{new}_{x,gro}\right]; \quad x = 1, ...M_{dv}, \quad (8)$$

$$Var^{new}_{x,gro} = \begin{cases} Var^{new}_{x,1,gro}, & if\ \beta < \frac{1}{M_{dv}}, \\ Var^{new}_{x,2,gro}, & if\ \frac{1}{M_{dv}} \le \beta < \frac{1}{M_{dv}} + 0.5, \\ Var^{new}_{x,gro}, & else, \end{cases} \quad (9)$$

where $Var^{new}_{x,1,gro}$and $Var^{new}_{x,2,gro}$are two x^{th} The random variables are chosen from the available pair; $Var^{new}_{x,gro}$ is a random number between 0 and 1, representing the range of values for which the random generator was responsible. The following is an illustration of how well the new solution works FF_{new}

Step 7. Eliminate the worst option and replace it with a better one.

Step 6 involves comparing the newly discovered solutions for each group Co^{worst}_{gro} The group's least effective option is evaluated to determine whether it should be abandoned in favour of a more recent and superior alternative discovered solution. To achieve a decision, the following analysis will be used:

$$Co^{worst}_{p} = \begin{cases} Co^{worst}_{gro}, & if\ FF^{worst}_{gro} < FF^{new}_{gro}, \text{group}\ Co^{worst}_{gro} \\ Co^{new}_{gro}, & else. \end{cases} \quad (10)$$

Step 8. COA employs solution trading among M_{gro} Ng groups to increase the number of viable solutions and M_{gro} prevent early convergence owing to local optimality zones. After each group has provided a solution, we will have them switch roles. The challenge is conducted using the following randomization method:

$$\varphi < \frac{10^{-2}}{2} M^2_{Co} \text{ among } M_{gro} \quad (11)$$

Algorithm 1
Birth, death inside a pack.

1: Compute ω and ϕ.
2: if $\phi = 1$ then
3: The sole coyote in the neighbourhood is killed, but the pup survives. ω
4: elseif $\phi > 1$ then
5: The pup survived the death of the area's youngest coyote ω
6: else ω dies
7: The pup dies.
8: end if

where ϕ Any integer between 0 and 1 in the wild is represented by. If the requirement in Eq. (11) is met, the solution exchange operation will be carried out. It should come as no surprise in each group influences the dynamics of solution exchange. As the number grows, the M_{co} possibility of two distinct solutions grows.

Step 9. Choose the most effective solution to the problemCo_{Gbest} higher M_{co}, solution Co_{Gbest}

Prior to each calculation iteration, the fitness functions of both groups are compared to determine the best Ng solution. If this is the final iteration, the best solution Co_{Gbest} will be chosen among the options developed during this run. In order to keep the coyote population stable, the COA maintains a balance between numbers of births and deaths, as demonstrated by the Algorithm 1 equation.

3.3.1. Improved coyote optimization algorithm

iteration is $\left(M_{Co} \times M_{gro} + 1 \times M_{gro}\right)$ equalling to $\left(M_{pop} + M_{gro}\right)$

According to Eqs. (4) and (5), each COA cycle provides two generations (5). (5). (8). In the first generation, all solutions for all groups are updated to the most recent version; however, in the second generation, only one solution for all groups is fully new. Following each cycle, $(M_{Co} \times M_{gro} + 1 \times M_{gro})$ new solutions, or an equal number of $(M_{pop} + M_{gro})$, are produced. The innovative method to generating solutions in the first generation improves the quality of the final output. However, the conventional COA approach for the first generation has some disadvantages. To prevent COA from spreading into so-called locally optimum zones, the second generation must create a unique solution for each group. Randomization is used to provide a unique answer, but it requires a large amount of data to account for the various components and calculations required to generate or pick each variable at random. As a result, we recommend revising the first two versions of the COA.

3.3.2. The first modification in the first generation

As the first stage in upgrading the system, select the response in the centre of Eq. (4) and replace it with the best response from the full audience. The core solution, which resolves the benchmark optimization functions, has a large influence on the MCOA technique for selecting the optimal solution. These observations can help determine the solution's position in the formula. There are numerous benchmark function optimal solutions between the lower and upper bounds of the interval 0. There are no answers for square, spherical, restrain, sum, or Rosen Brock. Because the values provided by these variables are so useful for finding new step sizes, group-cantered solutions typically contain variables close to zero. The areas between the lower and upper borders are insufficient to remedy the existing problem. As a result, exceptional solutions are generated, with the backup solution serving as the primary solution. As a result, we advocate replacing ineffective treatments with those that are more suited to the current population. Algorithm 2 is used to decipher the pseudocode of the COA. As a result, the following improvements have been made to the new solution-creation method:

$$Co^{new}_{p,gro} = Co_{p,gro} + [\gamma.(Co_{best,g} - Co_{1,gro}) + \gamma.(Co_{best,g} - Co_{2,gro})] \quad (12)$$

Algorithm 2
Pseudo code of the COA.

```
1: Initialize Mg packs with coyotes each
2: Verify the coyote's adaptation
3: while stopping criterion is not achieved do
4: for each p pack do
5: Define the alpha coyote of the pack
6: Compute the social tendency of the pack
7: for each c coyotes of the p pack do
8: Update the social condition
9: Evaluate the new social condition
10: Adaptation
11: end for
12: Birth and death (Alg.1).
13: end for
14: Transition between packs
15: Update the coyotes' ages.
16: end while
17: Select the best adapted coyote.
```

The following shortcomings in the supplied method can be mitigated slightly by employing the specific strategy:

Each MCOA solution contains a number of selection criteria, which must first be grouped before sorting. As a result, sorting each variable from each response is simplified. As a result, removing every potential solution variable becomes easier. The last step is to use mathematics to calculate the optimum selection criterion (7). If the number provided is exceptionally huge, the work will take an extremely lengthy time to finish. There will be more groups, which means that the centre solutions will take longer to implement.

3.3.3. The second generation's second modification

The secondly alteration that has to be made is a modification to the process that will be utilised to develop new solutions for the second generation. This is the second change that needs to be made. It is feasible to demonstrate, by making use of an Eq. (9). This can be done by saying that it is possible to demonstrate this. Based on how many decision elements there are, there are three possible decision outcomes, and each of these conditions include a random condition as well as variables that were chosen at random. The criteria themselves, in addition to the variables that are chosen, are chosen at random. In addition, random variables that are between the upper There are third selection condition bounds provided. For the first two criteria, two variables are chosen at random from two probable solutions. In the third condition, however, random variables are used within limitations that have already been established. It is glaringly obvious that the confluence of forces cannot produce high-quality, effective solutions. As a result, for the second enhancement, we suggest updating new solutions using two models that are based on the equations that are shown below:

$$CE_{gro} = Co_{Gbest} + \gamma^{*}(Co_{Gbest} - Co_{best,1}) + \gamma^{*}(Co_{Gbest} - Co_{best,2}) \tag{13}$$

$$CE_{gro} = Co_{Gbest} + \gamma^{*}(Co_{Gbest} - Co_{best,1}) + \gamma^{*}(Co_{Gbest} - Co_{best,2}) + \gamma^{*}(Co_{Gbest} - Co_{best,3}) \tag{14}$$

A comparison of the two sets of results shows that the answers obtained by (14) and those discovered using the first set of data differ significantly. It is unknown whether Eq. (14) can produce higher-quality answers in the absence of a fitness-determining technique. Because Eq. (13) yields a result that is similar to the previous one, the search for the local optimal solution may fail. If the third step size in Eq. (14) is also large, the incidence repeats the new solution will finally arrive to a region that is significantly different from the starting region. This is due to the fact that the distribution of the new solution between zones will be highly variable. Thus, depending on how Eq. (14) is implemented, the local search approach may be less effective. This is true if the context is proper. When there are considerable discrepancies in the solutions presented, the issue usually becomes apparent after a few iterations. Because the answers examined by Eq. (14) are comparable, this strategy works best when there are many repetitions or when the procedure is nearly complete. Before selecting whether or not to hire, you must have a legitimate reason (14). We recommend comparing the two sets of solutions to evaluate the fitness functions of each set's responses and determine which equation works best under the given circumstances. When several solutions are somewhat close to one another, significant steps are taken. Starting slowly can be an effective strategy. The total number of solution pairs is divided by the number of solution pairs that are narrowly spaced apart. If the ratio is high enough to show that many responses are quite similar, the leaping step should be decided using the closest responses (14). We use a pseudocode to compute the value of Count, which stands for the number of solution-pairs that are close to one another in this situation. The words Count max and B, derived from Eq. (15) and (B), can also be used to express the ratio and the maximum number of closely spaced solutions in pairs (16). Higher values of B, which range from 0 to 1, indicate closer solutions, as shown by Eq (16). When B is very close to one, virtually all of the solutions are close to one another; when B is very close to zero, almost none of the solutions are. As a result, it must compute the Pa probability for each optimization issue Pa is quite tall to allow the application of Eq. (14) with a significant step size. In all other cases, the questioned instances are eliminated if the Eq. (13) is employed. To arrive at numerical findings, we first examine how different Pa values affect the output. Then we recommend the Pa value that feels most appropriate.

$$Count_{\max} = \frac{M_{Co} \times (M_{Co} + 1)}{2} \tag{15}$$

$$B = \frac{Count}{Count_{\max}} \tag{16}$$

4. Result and discussion

Python 3.6 can be used to test the functionality of the proposed framework. Keras and Tensor Flow were used to implement machine learning and deep learning models. This study compares the proposed MPNN-MCOA approach against five alternative machine learning algorithms: LSTM (Long Short-Term Memory), KNN (K-Nearest Neighbour), CNN (Convolutional Neural Network), RFNN (Radial Basis NN) as well as ARIMA

4.1. Evaluation metrics

The classification results are displayed in the confusion matrix (29). The confusion matrix supports practitioners in identifying if the outcomes have a high-performance level. Patients with heart disease who were correctly diagnosed were categorised as true positives (TPs), while those without the disease were categorised as true negatives (TNs), while those with heart disease were categorised as false negatives (FNs) and those without heart disease were categorised as false positives (FPs). False negative projections are the most destructive in the field of medicine. The various performance measures were derived using a confusion matrix. Accuracy was computed based on instances with proper identification (Acc). Eq. (17) gives the formula for calculating accuracy (17).

$$Accuracy = \frac{TP + TN}{TP + TN + FP + FN} \tag{17}$$

Precision: It is measured using the ratio of true positive pixels to the sum of true positive and false positive pixels and is calculated using Eq. (18):

$$\Pr ecision = \frac{TP}{TP + FP} \tag{18}$$

Recall: It is calculated by comparing true positive pixels to the sum of true positive and false negative pixels.

$$Recall = \frac{TP}{TP + FN} \tag{19}$$

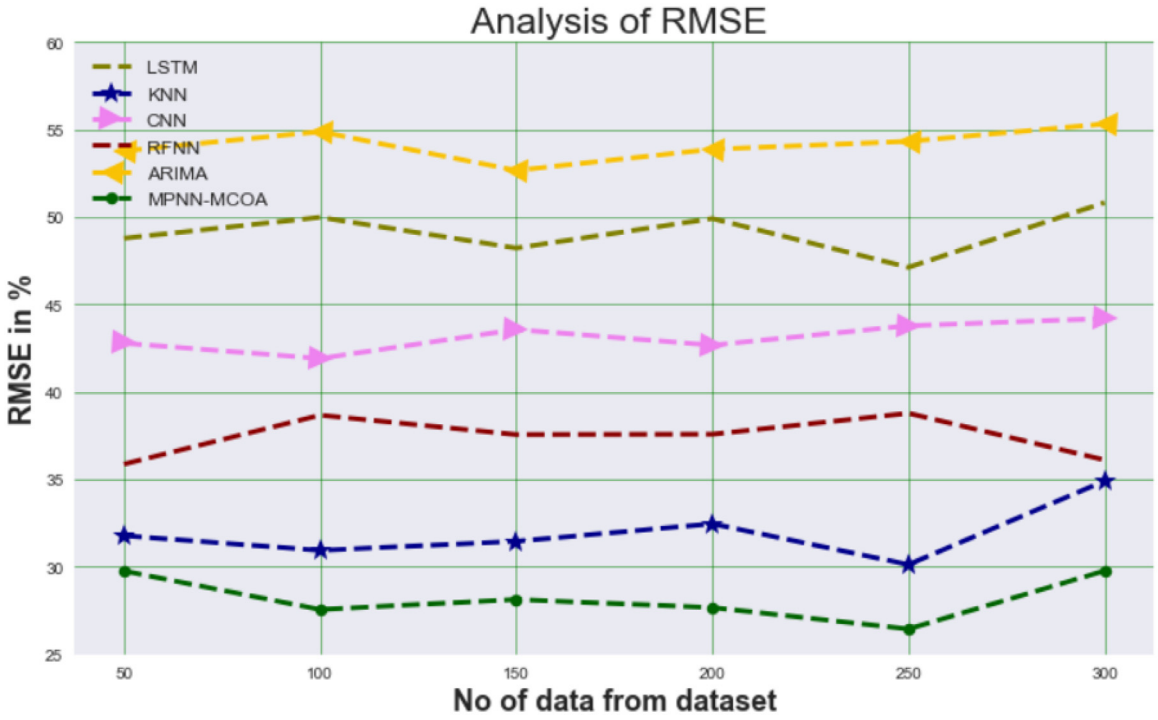

Fig. 3. RMSE analysis for MPNN-MCOA method with existing systems.

F1 Score: This score, which indicates the system's overall performance, is calculated using Eq. (20)

$$F - Score = 2 * \frac{precision * recall}{precision + recall} \tag{20}$$

True-positive (TP) pixels accurately identify an ear; false-positive (FP) pixels correctly identify non-ear (non-ear) pixels; and false-negative (FN) pixels incorrectly classify the backdrop as an ear. These three abbreviations distinguish three sorts of ear pixels. Because there is only one class, it is impossible to identify ears.

Error-Quadratic Root of Mean

Only the existence of a square root sign (Tatar et al., 2016) separates it from MSE; otherwise, it is identical. The sign of the mean absolute error equation is (21).

$$RMSE = \sqrt{\sum_{i=1}^{n} \frac{\left(\hat{y}_i - y_i\right)^2}{n}} \tag{21}$$

Root mean squared error (RMSE) takes the values from 0 to ∞, and the smaller RMSE values are desirable (Sedghamiz et al., 2015).

Absolute error in percentage mean

Mean absolute percentage error

By adding the word "%" to the term "mean absolute error," the term "mean absolute percentage error" (MAPE) is defined.

$$MAPE = \frac{100}{n} \sum_{i=1}^{n} \left| \frac{y_i - \hat{y}_i}{y_i} \right| \tag{22}$$

If the MAPE score is lesser than 10%, the forecast is considered "very accurate."

If the MAPE's score is between 10% and 20%, the forecast's accuracy is considered "good."

If the MAPE is between 20% and 50%, the accuracy of the forecast is considered "moderate."

In addition, the forecast - categorised as "inaccurate prediction accuracy" if MAPE score exceeds 50% (Hosseinzadeh et al., 2021).

4.1.1. RMSE(Root mean square error)

In Fig. 3 and Table 2, the MPNN-MCOA strategy is contrasted with several current approaches. The graph shows how machine learning has increased performance while decreasing RMSE. For example, with data size 50, the RMSE value is 29.76% for MPNN-MCOA, whereas the LSTM, KNN, CNN, RFNN, and ARIMA models have obtained slightly enhanced RMSE of 48.78%, 31.78%, 42.78%, 35.87%, and 53.78%, respectively. However, the MPNN-MCOA model has shown maximum performance for different data sizes with low RMSE values. Similarly, under 300 data points, the RMSE value of MPNN-MCOA is 29.77%, while it is 50.82%, 34.91%, 44.19%, 36.11%, and 55.31% for LSTM, KNN, CNN, RFNN, and ARIMA models, respectively.

4.1.2. MAPE (Mean absolute percentage error)

Fig. 4 depicts a MAPE comparison of the MPNN-MCOA technique and other existing approaches, with the findings summarised in Table 3. The accompanying graph indicates that using a machine learning technique directly improves both performance and the MAPE value. For example, with data size 50, the MAPE value is 32.65% for MPNN-MCOA, whereas the LSTM, KNN, CNN, RFNN, and ARIMA models have obtained slightly enhanced MAPE of 43.23%, 39.67%, 55.23%, 52.13%, and 36.87%, respectively. However, the MPNN-MCOA model has shown maximum performance for different data sizes with low MAPE values. Similarly, under 300 data points, the MAPE value of MPNN-MCOA is 35.61%, while it is 46.56%, 43.51%, 60.56%, 54.67%, and 38.19% for LSTM, KNN, CNN, RFNN, and ARIMA models, respectively.

4.1.3. NRMSE (Normalized root mean square error)

In Fig. 5 and Table 4, the NRMSE findings achieved using the MPNN-MCOA approach are compared to those obtained with other, more traditional methods. The system's performance and NRMSE value have both improved significantly as a result of the use of a machine learning technique. For example, with data size 50, the NRMSE value is 41.67% for MPNN-MCOA, whereas the LSTM, KNN, CNN, RFNN, and ARIMA models have obtained slightly enhanced NRMSE of 70.34%, 63.45%, 59.18%, 55.46%, and 48.78%, respectively. However, the MPNN-MCOA model has shown maximum performance for different

Table 2
RMSE analysis for MPNN-MCOA method with existing systems.

No of data from dataset	LSTM	KNN	CNN	RFNN	ARIMA	MPNN-MCOA
50	48.78	31.78	42.78	35.87	53.78	29.76
100	49.98	30.94	41.91	38.67	54.87	28.56
150	48.22	31.46	43.56	37.56	52.66	28.13
200	49.91	32.46	42.67	37.58	53.87	27.67
250	47.12	30.13	43.78	38.78	54.32	26.45
300	50.82	34.91	44.19	36.11	55.31	29.77

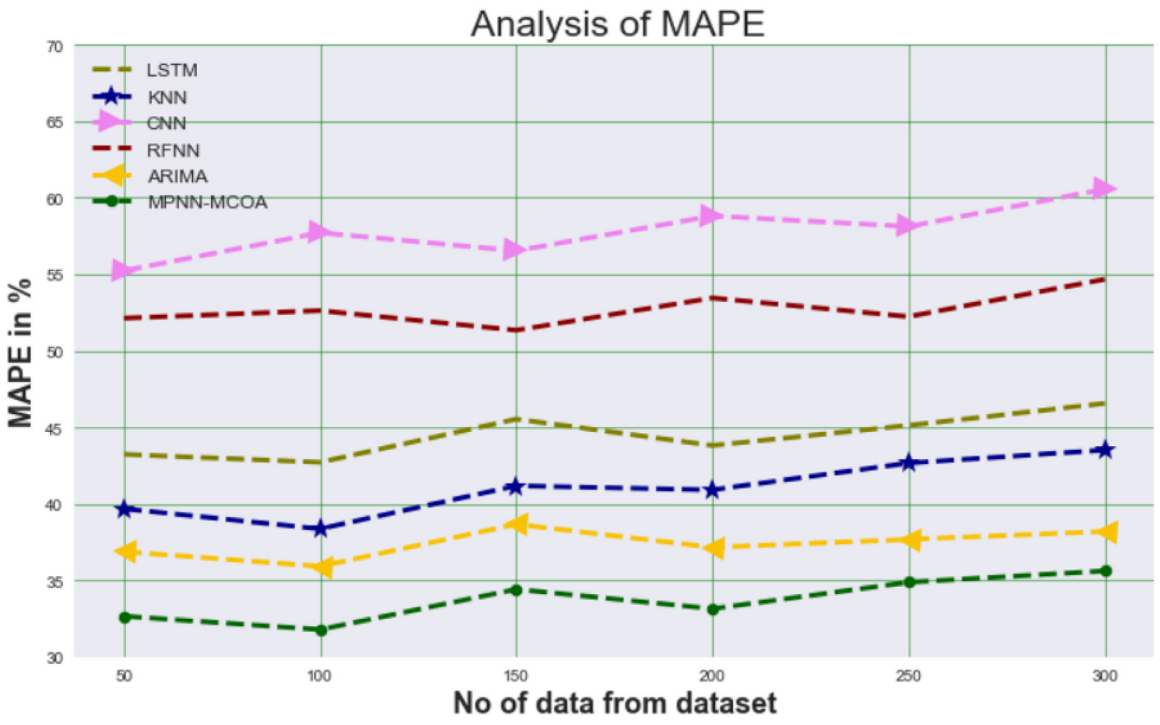

Fig. 4. MAPE analysis for MPNN-MCOA method with existing systems.

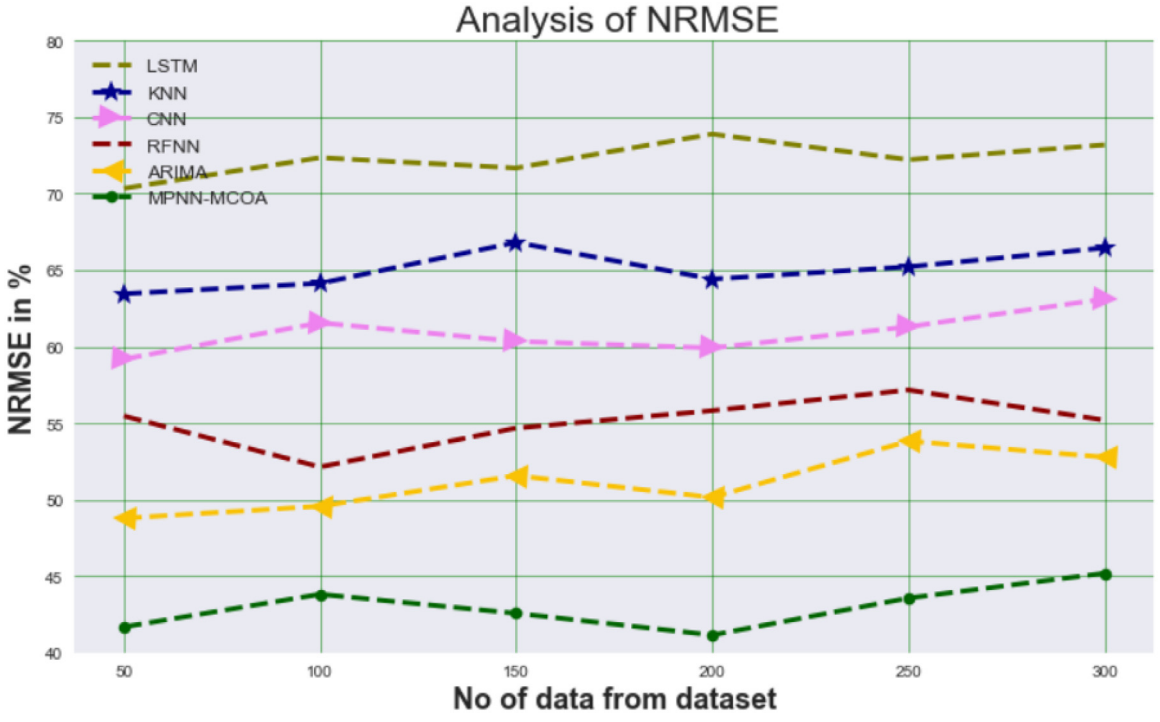

Fig. 5. NRMSE analysis for MPNN-MCOA method with existing systems.

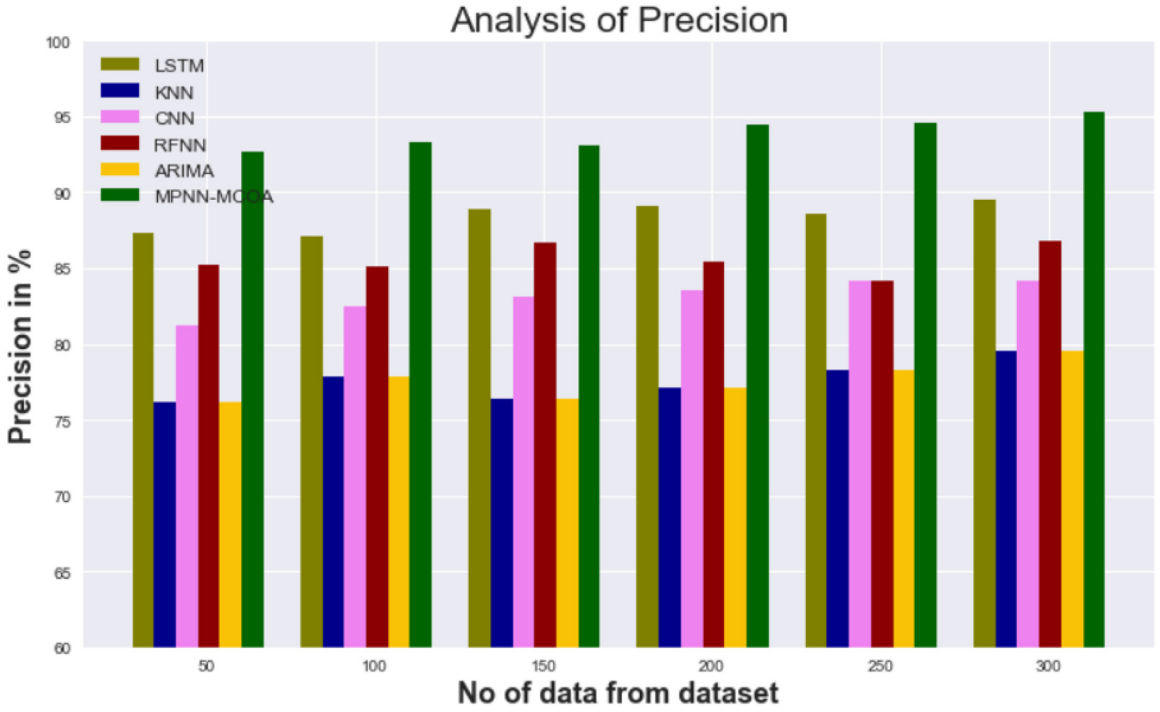

Fig. 6. Precision analysis for MPNN-MCOA method with existing systems.

Table 3
MAPE analysis for MPNN-MCOA method with existing systems.

No of data from dataset	LSTM	KNN	CNN	RFNN	ARIMA	MPNN-MCOA
50	43.23	39.67	55.23	52.13	36.87	32.65
100	42.71	38.36	57.71	52.62	35.91	31.78
150	45.53	41.17	56.53	51.34	38.66	34.41
200	43.81	40.91	58.81	53.45	37.15	33.14
250	45.12	42.66	58.12	52.23	37.67	34.87
300	46.56	43.51	60.56	54.67	38.19	35.61

Table 4
NRMSE analysis for MPNN-MCOA method with existing systems.

No of data from dataset	LSTM	KNN	CNN	RFNN	ARIMA	MPNN-MCOA
50	70.34	63.45	59.18	55.46	48.78	41.67
100	72.34	64.13	61.55	52.13	49.56	43.81
150	71.67	66.81	60.34	54.67	51.56	42.56
200	73.89	64.41	59.91	55.81	50.14	41.14
250	72.21	65.21	61.29	57.16	53.82	43.56
300	73.18	66.45	63.11	55.19	52.77	45.18

Table 5
Precision analysis for MPNN-MCOA method with existing systems.

No of data from dataset	LSTM	KNN	CNN	RFNN	ARIMA	MPNN-MCOA
50	87.34	76.13	81.23	85.23	76.13	92.67
100	87.11	77.89	82.44	85.12	77.89	93.25
150	88.89	76.41	83.13	86.67	76.41	93.14
200	89.13	77.12	83.56	85.45	77.12	94.45
250	88.56	78.31	84.15	84.12	78.31	94.56
300	89.56	79.56	84.11	86.78	79.56	95.33

Table 6
Recall analysis for MPNN-MCOA method with existing systems.

No of data from dataset	LSTM	KNN	CNN	RFNN	ARIMA	MPNN-MCOA
50	77.13	71.89	65.56	84.21	83.12	91.45
100	78.34	72.78	65.13	85.41	84.65	92.77
150	79.21	73.56	66.67	85.37	85.16	91.32
200	80.51	74.71	67.89	86.13	83.31	92.89
250	81.23	75.21	68.34	87.68	84.15	93.15
300	82.76	76.97	69.21	88.79	83.91	94.11

data sizes with low NRMSE values. Similarly, under 300 data points, the NRMSE value of MPNN-MCOA is 45.18%, while it is 73.18%, 66.45%, 63.11%, 55.19%, and 52.77% for LSTM, KNN, CNN, RFNN, and ARIMA models, respectively.

4.1.4. Precision

In Fig. 6 and Table 5 show the results of a precision comparison between the MPNN-MCOA strategy and a number of well-known strategies. As seen in the graph, using a machine learning-based solution improves both performance and accuracy. For example, with data size 50, the precision value is 92.67% for MPNN-MCOA, whereas the LSTM, KNN, CNN, RFNN, and ARIMA models have obtained precision of 87.34%, 76.13%, 81.23%, 85.23%, and 76.13%, respectively. However, the MPNN-MCOA model has shown maximum performance with different data sizes. Similarly, under 300 data points, the precision value of MPNN-MCOA is 95.33%, while it is 89.56%, 79.56%, 84.11%, 86.78%, and 79.56% for LSTM, KNN, CNN, RFNN, and ARIMA models, respectively.

4.1.5. Recall

Fig. 7 and Table 6 illustrate the results of a recall comparison between the MPNN-MCOA methodology and a variety of other well-known methodologies. The graph indicates an improvement in performance and recall, illustrating the usefulness of the machine learning technique. For example, with data 50, the recall value is 91.45% for MPNN-MCOA, whereas the LSTM, KNN, CNN, RFNN, and ARIMA models have obtained recalls of 77.13%, 71.89%, 65.56%, 84.21%, and 83.12%, respectively. However, the MPNN-MCOA model has shown maximum performance with different data sizes. Similarly, under 300 data points, the recall value of MPNN-MCOA is 94.11%, while it is 82.76%, 76.97%, 69.21%, 88.79%, and 83.91% for LSTM, KNN, CNN, RFNN, and ARIMA models, respectively.

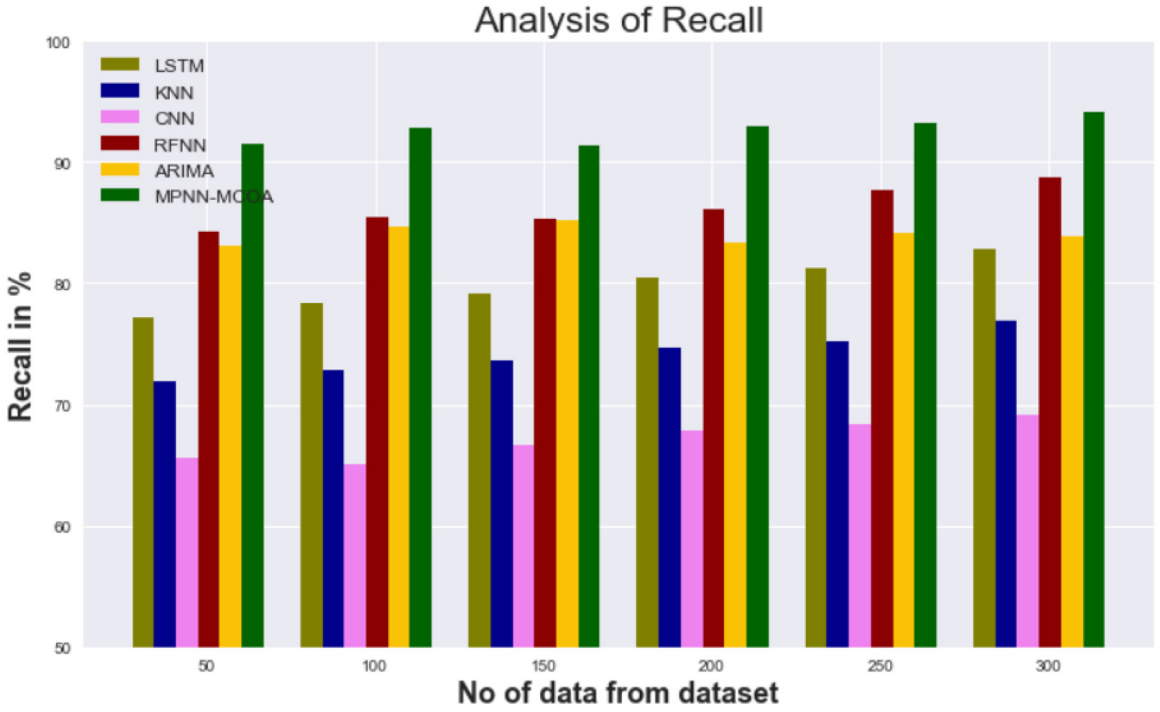

Fig. 7. Recall analysis for MPNN-MCOA method with existing systems.

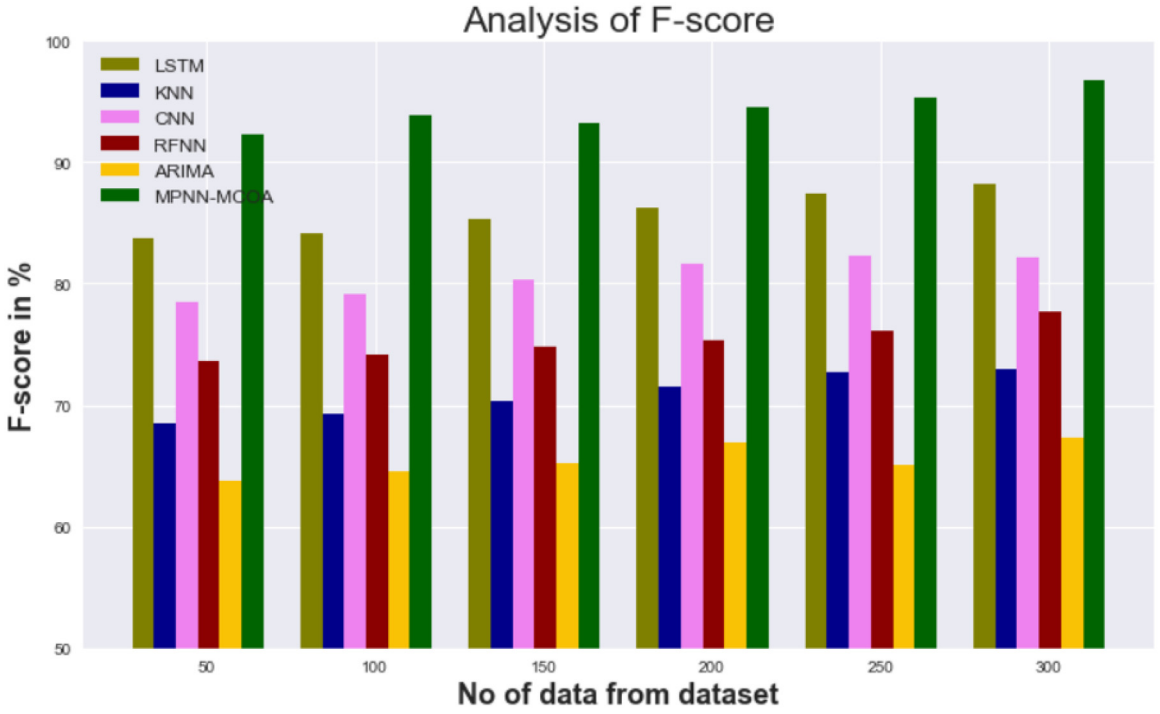

Fig. 8. F-score analysis for MPNN-MCOA method with existing systems.

4.1.6. F-Score

Fig. 8 and Table 7 illustrate the results of an f-score analysis comparing the MPNN-MCOA strategy to others already in use. A higher f-score on the graph indicates that the machine learning technique is now performing better. For example, with data 50, the f-score value is 92.31% for MPNN-MCOA, whereas the LSTM, KNN, CNN, RFNN, and ARIMA models have obtained f-scores of 83.78%, 68.46%, 78.46%, 73.67%, and 63.76%, respectively. However, the MPNN-MCOA model has shown maximum performance with different data set sizes. Similarly, under 300 data points, the f-score value of MPNN-MCOA is 96.71%, while it is 88.19%, 72.98%, 82.15%, 77.71%, and 67.31% for LSTM, KNN, CNN, RFNN, and ARIMA models, respectively.

4.1.7. Accuracy

Fig. 9 and Table 8 illustrate the results of a study comparing the accuracy of the MPNN-MCOA approach to that of competing systems. The graph depicts the rise in efficiency and accuracy brought about by the use of machine learning technologies. For example, with data 50, the accuracy value is 91.56% for MPNN-MCOA, whereas the LSTM, KNN, CNN, RFNN, and ARIMA models have obtained accuracy of

Table 7
F-score analysis for MPNN-MCOA method with existing systems.

No of data from dataset	LSTM	KNN	CNN	RFNN	ARIMA	MPNN-MCOA
50	83.78	68.46	78.46	73.67	63.76	92.31
100	84.16	69.31	79.21	74.12	64.57	93.87
150	85.31	70.35	80.31	74.78	65.21	93.15
200	86.18	71.46	81.67	75.39	66.87	94.56
250	87.45	72.67	82.33	76.16	65.12	95.31
300	88.19	72.98	82.15	77.71	67.31	96.71

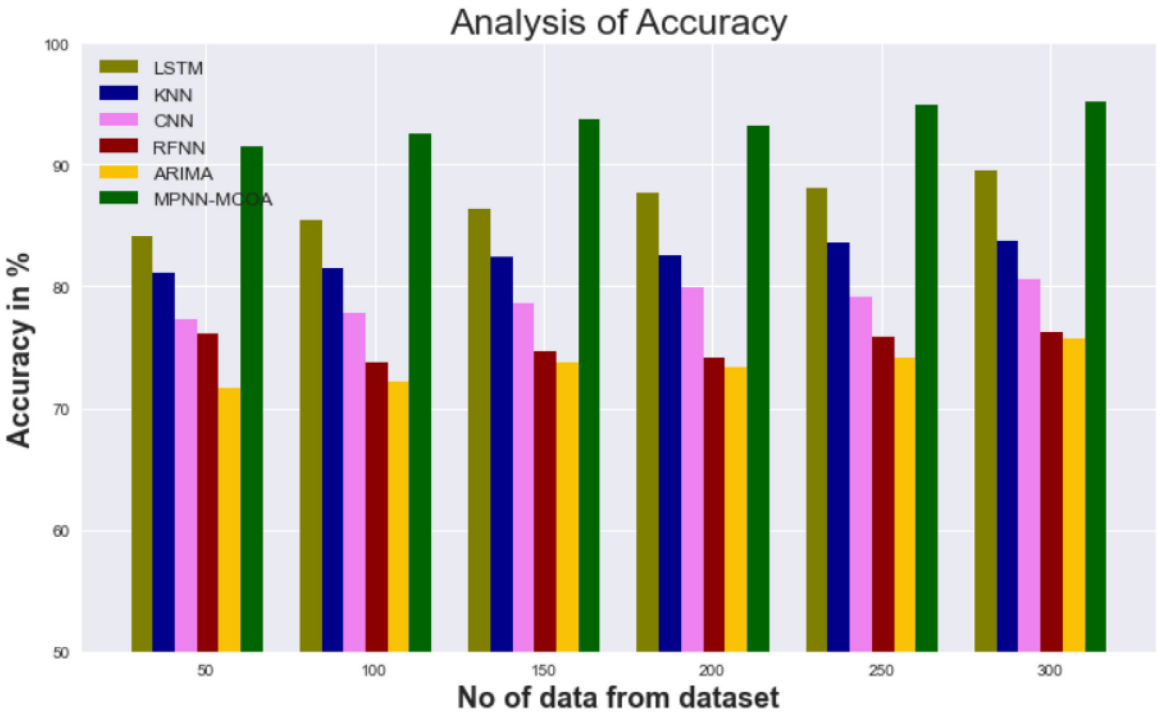

Fig. 9. Accuracy analysis for MPNN-MCOA method with existing systems.

Table 8
Accuracy Analysis for MPNN-MCOA method with existing systems.

No of data from dataset	LSTM	KNN	CNN	RFNN	ARIMA	MPNN-MCOA
50	84.16	81.14	77.31	76.13	71.67	91.56
100	85.45	81.56	77.89	73.78	72.12	92.56
150	86.31	82.37	78.56	74.67	73.78	93.67
200	87.68	82.56	79.91	74.21	73.39	93.16
250	88.11	83.67	79.14	75.89	74.16	94.87
300	89.59	83.77	80.56	76.31	75.71	95.13

84.16%, 81.14%, 77.31%, 76.13%, and 71.67%, respectively. However, the MPNN-MCOA model has shown maximum performance with different data sizes. Similarly, under 300 data points, the accuracy value of MPNN-MCOA is 95.13%, while it is 89.59%, 83.77%, 80.56%, 76.31%, and 75.71% for LSTM, KNN, CNN, RFNN, and ARIMA models, respectively.

5. Conclusion

Both the safety of India's inhabitants and the efficiency of its administration depend on a realistic prediction of the country's CO2 emissions over the coming decades. India is currently ranked second among countries with the highest CO2 production, according to the most recent data. Our contribution is to reduce CO2 emissions to save lives. In this research, the Modified Coyote Optimization Algorithm was utilised to extract the required characteristics. The empirical results showed that predictions made using the Multi-Layer Perceptron's Neural Network (MPNN) were more accurate than predictions made using other models. The MPNN-MCOA found a link between CO2 emissions, economic growth, and entrepreneurial opportunity. Governance, personal freedom, education, and pollution all have a negative association. however, the results obtained are not tested in the opposite situation is obtained with a greenhouse without cultivation is not tested with cultivation and vice versa. In addition, the models obtained can hardly be used in another type of greenhouse, so the generalization of the models should be a more relevant issue. In our conclusion, we emphasise the importance of machine learning (ML) in accelerating the transition to carbon neutrality, from MPNN-MCOA atomic simulations to global energy management. Indexes like RMSE, MAPE, NRMSE, and Accuracy were used to measure the precision, recall, and accuracy of machine learning algorithm predictions. Several machine learning algorithms' outputs are applied to a mathematical model using MPNN-MCOA algorithms. It offers a mathematical method for improving forecast precision. Using well-known models such as LSTM, KNN, CNN, RFNN, and ARIMA did not enhance prediction accuracy, according to this method (Autoregressive Integrated Moving Average). 95.13 percent of the time, the proposed

model accurately identified a user's membership in a category. Future research should examine a wider range of machine-learning models for this application and an important guideline for future works is the integration and exchange of information using 4.0 technologies. The role of the ANNs is to develop predictive models that take advantage of the information generated and its management.

Declaration of Competing Interest

The authors declare that they have no known competing financial interests or personal relationships that could have appeared to influence the work reported in this paper.

Data availability

Data will be made available on request.

Funding

The authors received no specific funding for this Research.

References

Ahmadi, P., 2019. Environmental impacts and behavioral drivers of deep decarbonization for transportation through electric vehicles. J. Clean. Prod. 225, 1209–1219.
Bakay, M.S., Agbulut, Ü., 2021. Electricity production based forecasting of greenhouse gas emissions in Turkey with deep learning, support vector machine and artificial neural network algorithms. J. Clean. Prod. 285, 125324 Article.
Cao, H., Lin, T., Li, Y., Zhang, H., 2019. Stock Price Pattern Prediction Based on Complex Network and Machine Learning. Complexity 2019, 01–12 vol.
Daryayehsalameh, B., Nabavi, M., Vaferi, B., 2021. Modeling of CO2 capture ability of [Bmim][BF4] ionic liquid using connectionist smart paradigms. Environ. Technol. Innov. 22, 101484.
Dwivedi, Y.K., Hughes, L., Kar, A.K., Baabdullah, A.M., Grover, P., Abbas, R., Wade, M., 2022. Climate change and COP26: are digital technologies and information management part of the problem or the solution? An editorial reflection and call to action. Int. J Inf. Manag. 63, 102456 Article.
Fang, X., Liu, W., Ai, J., He, M., Wu, Y., Shi, Y., Shen, W., Bao, C., 2020. Forecasting incidence of infectious diarrhea using random forest in Jiangsu Province. China BMC Infect. Dis. 20 (1), 1–8.
Fernández, Y.F., López, M.F., Blanco, B.O., 2018. Innovation for sustainability: the impact of R&D spending on CO2 emissions. J. Clean.Prod. 172, 3459–3467.
Hamrani, A., Akbarzadeh, A., Madramootoo, C.A., 2020. Machine learning for predicting greenhouse gas emissions from agricultural soils. Sci. Total Environ. 741, 140338 Article.
Hosseinzadeh, M., Ahmadi, A., Foroushani, M.S., 2021. Developing the dynamic model of earthquake crisis management in tehran city using system dynamics approach. J. Nat. Environ. Hazards 10, 67–90 27.
Javadi, P., Yeganeh, B., Abbasi, M., Alipourmohajer, S., 2021. Energy assessment and greenhouse gas predictions in the automotive manufacturing industry in Iran. Sustain. Prod. Consum. 26, 316–330.
Keith, D.W., Holmes, G., Angelo, D.S., Heidel, K., 2018. A process for capturing CO2 from the atmosphere. Joule 2, 1573–1594.
Kjellstrom, T., 2016. Impact of climate conditions on occupational health and related economic losses: a new feature of global and urban health in the context of climate change. Asia Pac. J. Public Health 28 (2), 28S–37S Suppl.
Lepore, A., dos Reis, M.S., Palumbo, B., Rendall, R., Capezza, C., 2017. A comparison of advanced regression techniques for predicting ship CO2 emissions. Qual. Reliab. Eng. Int. 33 (6), 1281–1292.
Li, M., Wang, W., De, G., Zi, X., Tan, Z., 2018. Forecasting carbon emissions related to energy consumption in Beijing-Tianjin-Hebei region based on grey prediction theory and extreme learning machine optimized by support vector machine algorithm. Energies 11 (9), 247.
Magazzino, C., Mele, M., Morelli, G., Schneider, N., 2021. The nexus between information technology and environmental pollution: application of a new machine learning algorithm to OECD countries. Util. Policy 72, 101256.
Mesbah, M., Shahsavari, S., Soroush, E., Rahaei, N., Rezakazemi, M, 2018. Accurate prediction of miscibility of CO2 and supercritical CO2 in ionic liquids using machine learning. J. CO2 Util. 25, 99–107.
Mostafaeipour, A., Bidokhti, A., Fakhrzad, M.B., Sadegheih, A., Mehrjerdi, Y.Z., 2022. A new model for the use of renewable electricity to reduce carbon dioxide emissions. Energy 238, 121602 Article.
Niu, D., Wang, K., Wu, J., Sun, L., Liang, Y., Xu, X., Yang, X., 2020. Can China achieve its 2030 carbon emissions commitment? Scenario analysis based on an improved general regression neural network. J. Clean. Prod. 243, 118558 Article.
Olanrewaju, O.A., Mbohwa, C., 2017. Assessing potential reduction in greenhouse gas: an integrated approach. J. Clean. Prod. 141, 891–899.
Ouaer, H., Hosseini, A.H., Nait Amar, M., El Amine Ben Seghier, M., Ghriga, M.A., Nabipour, N., Shamshirband, S., 2019. Rigorous connectionist models to predict carbon dioxide solubility in various ionic liquids. Appl. Sci. 10, 304.
Romeo, L.M., Minguell, D., Shirmohammadi, R., Andrés, J.M., 2020. Comparative analysis of the efficiency penalty in power plants of different amine-based solvents for CO2 capture. Ind. Eng. Chem. Res. 59, 10082–10092.
Samal, K.K.R., Panda, A.K., Babu, K.S., Das, S.K., 2021. An improved pollution forecasting model with meteorological impact using multiple imputation and finetuning approach. Sustain. Cities Soc. 70, 102923 Article.
Sedghamiz, M.A., Rasoolzadeh, A., Rahimpour, M.R., 2015. The ability of artificial neural network in prediction of the acid gases solubility in different ionic liquids. J. CO2 Util. 9, 39–47.
Shabani, E., Hayati, B., Pishbahar, E., Ghorbani, M.A., Ghahremanzadeh, M., 2021. A novel approach to predict CO2 emission in the agriculture sector of Iran based on inclusive multiple model. J. Clean. Prod. 279, 123708 Article.
Shaikh, M.A., Kucukvar, M., Onat, N.C., Kirkil, G., 2017. A framework for water and carbon footprint analysis of national electricity production scenarios. Energy 139, 406–421.
Song, Z., Shi, H., Zhang, X., Zhou, T., 2020. Prediction of CO2 solubility in ionic liquids using machine learning methods. Chem. Eng.Sci. 223, 115752.
Tatar, A., Naseri, S., Bahadori, M., Hezave, A.Z., Kashiwao, T., Bahadori, A., Darvish, H., 2016. Prediction of carbon dioxide solubility inionic liquids using MLP and radial basis function (RBF) neural networks. J. Taiwan Inst. Chem. Eng. 60, 151–164.
Wang, Z.X., Ye, D.J., 2017. Forecasting Chinese carbon emissions from fossil energy consumption using non-linear grey multivariable models. J. Clean. Prod. 142, 600–612.
Wang, Q., Li, S., Pisarenko, Z., 2020. Modeling carbon emission trajectory of China, US and India. J. Clean. Prod. 258, 120723.
Yang, H., O'Connell, J.F., 2020. Short-term carbon emissions forecast for aviation industry in Shanghai. J. Clean. Prod. 275, 122734 Article.
Zeng, S., Zhang, X., Bai, L., Zhang, X., Wang, H., Wang, J., Zhang, S., 2017. Ionic-liquid-based CO2 capture systems: structure, interaction and process. Chem. Rev. 117, 9625–9673.